Cell Cycle-Dependent Binding Modes of the Ran Exchange Factor RCC1 to Chromatin

Martin Bierbaum[†‡] and Philippe I. H. Bastiaens[†‡]*

[†]Department of Systemic Cell Biology, Max Planck Institute for Molecular Physiology, Dortmund, Germany; and [‡]Faculty of Chemistry, Technical University Dortmund, Dortmund, Germany

Submitted June 15, 2012, and accepted for publication March 11, 2013.

*Correspondence: philippe.bastiaens@mpi-dortmund.mpg.de

1 Supplementary information

1.1 The binding-diffusion model

In the following we derive a model for the analysis of binding reactions by FCS following and extending an approach originally developed by Elson and Magde [1]. The basic biological assumption of this model is that proteins can either freely diffuse or can be immobilized by binding to specific binding sites (see figure S1). Diffusion is assumed to follow Fick's law, while binding is modelled as a single-step bimolecular binding reaction. This reaction-diffusion system can be described by a system of differential equations:

$$\begin{aligned} \frac{\partial[A]}{\partial t} &= D\nabla^2[A] - k_{\text{on}}[B][A] + k_{\text{off}}[AB] \\ \frac{\partial[B]}{\partial t} &= -k_{\text{on}}[B][A] + k_{\text{off}}[AB] \\ \frac{\partial[AB]}{\partial t} &= k_{\text{on}}[B][A] - k_{\text{off}}[AB] \end{aligned} \tag{1}$$

where $[A]$ is the concentration of unbound proteins, $[B]$ is the concentration of available binding sites, and $[AB]$ is the concentration of the AB complex. D is the diffusion constant of A, ∇^2 is the Laplacian operator, k_{on} is the association rate constant, and k_{off} is the dissociation rate constant.

To simplify eq. (1), the concentration of binding sites, $[B]$, is assumed to be much larger than the concentration of binding partners, $[A] + [AB]$. Under this condition, changes in $[B]$ due to binding can be neglected and $[B]$ can be assumed to be constant. This eliminates the second equation from eq. (1) and also introduces a pseudo-first-order association rate constant $k_{\text{on}}[B]$.

1.2 Derivation

1.2.1 The concentration correlation function

The first step in calculating the fluorescence autocorrelation function is to calculate the concentration correlation function. For a system of m labelled components, the concentration correlation function, $\phi_{jl}(\mathbf{r}, \mathbf{r}', t)$, compares the concentration fluctuations of component j at position $\mathbf{r}$ to the concentration fluctuation of component l at position $\mathbf{r}'$ and after time τ:

$$\phi_{jl}(\mathbf{r}, \mathbf{r}', \tau) = \langle \delta C_j(\mathbf{r}, 0) \delta C_l(\mathbf{r}', \tau) \rangle \tag{2}$$

Here, $\delta C_l(\mathbf{r}, \tau) = C_l(\mathbf{r}, \tau) - \langle C_l \rangle$ is the local deviation from the average concentration $\langle C_l \rangle$.

If the δC_l are small with respect to the equilibrium concentrations, chemical rate equations such as those in eq. (1) can be used to describe the relaxation of the δC_l. In general terms, the system of differential equations for the δC_l can be written as:

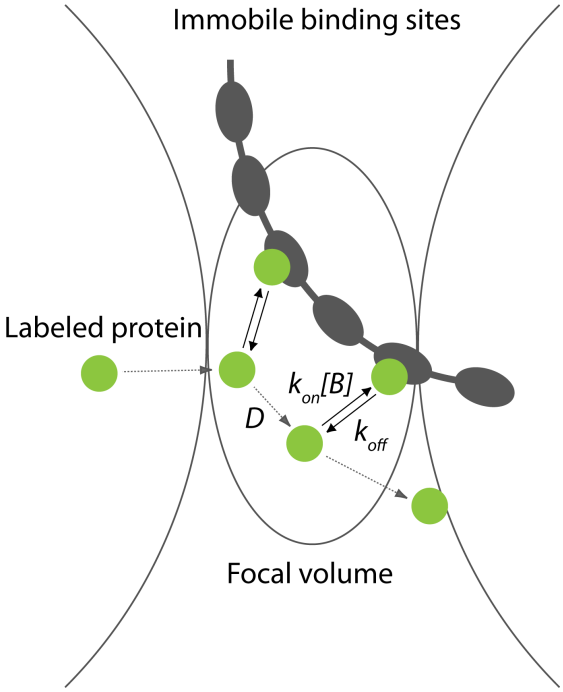

Figure S1: Schematic depiction of the binding-diffusion model. The diffusion constant D describes the labelled protein's diffusion, while the association rate constant $k_{\mathrm{on}}[B]$ and the dissociation rate constant k_{off} describe the transient interaction with immobile binding sites. The confocal observation volume, from which the fluorescence fluctuations are observed, is modelled by a three-dimensional Gaussian.

$$\frac{\partial \delta C_l(\mathbf{r},\tau)}{\partial \tau} = D_l \nabla^2 \delta C_l(\mathbf{r},\tau) + \sum_{k=1}^{m} T_{lk} \delta C_k(\mathbf{r},\tau) \tag{3}$$

Here, the matrix elements T_{lk} are the chemical rate constants and the equilibrium concentrations of the components, and D_l is the diffusion constant of component l.

To calculate ϕ_{jl}, eq. (3) needs to be solved for the $\delta C_l(\mathbf{r},\tau)$. This is achieved by Fourier-transformation, which transforms eq. (3) into:

$$\frac{\partial \tilde{C}_l(\mathbf{q},\tau)}{\partial \tau} = \sum_{k=1}^{m} M_{lk} \tilde{C}_k(\mathbf{q},\tau) \tag{4}$$

where $\tilde{C}_l(\mathbf{q},\tau) = (2\pi)^{-3/2} \int d^3\mathbf{r}\, e^{i\mathbf{qr}} \delta C_l(\mathbf{r},\tau)$ is the Fourier-transformation of $\delta C_l(\mathbf{r},\tau)$, and $M_{lk} = T_{lk} - D_l \mathbf{q}^2 \delta_{lk}$. For the particular binding-diffusion system in eqs. (1) with the two species A and C, the matrix M is:

$$M = \begin{pmatrix} -k_{\mathrm{on}}[B] - \mathbf{q}^2 D & k_{\mathrm{off}} \\ k_{\mathrm{on}}[B] & -k_{\mathrm{off}} \end{pmatrix} \tag{5}$$

The solution of the system in eq. (4) is expressed through the eigenvalues $\lambda^{(s)}$ and the matrix of eigenvectors X of the matrix M:

$$\tilde{C}_l(\mathbf{q},\tau) = \sum_{s=1}^{m} X_l^{(s)} e^{\lambda^{(s)}\tau} \sum_{k=1}^{m} (X^{-1})_k^{(s)} \tilde{C}_k(\mathbf{q},0) \tag{6}$$

This result is inserted into eq. (2), and Fourier-synthesis is performed:

$$\begin{aligned}
\phi_{jl}(\mathbf{r},\mathbf{r}',\tau) &= (2\pi)^{-3/2} \int d^3\mathbf{q}\, e^{-i\mathbf{qr}'} \langle \delta C_j(\mathbf{r},0) \tilde{C}_l(\mathbf{q},\tau) \rangle \\
&= (2\pi)^{-3/2} \int d^3\mathbf{q}\, e^{-i\mathbf{qr}'} \sum_{s=1}^{m} X_l^{(s)} e^{\lambda^{(s)}\tau} \sum_{k=1}^{m} (X^{-1})_k^{(s)} \langle \delta C_j(\mathbf{r},0) \tilde{C}_k(\mathbf{q},0) \rangle \\
&= (2\pi)^{-3} \int d^3\mathbf{q}\, e^{-i\mathbf{qr}'} \sum_{s=1}^{m} X_l^{(s)} e^{\lambda^{(s)}\tau} \sum_{k=1}^{m} (X^{-1})_k^{(s)} \int d^3\mathbf{r}''\, e^{i\mathbf{qr}''} \langle \delta C_j(\mathbf{r},0) \delta C_k(\mathbf{r}'',0) \rangle
\end{aligned} \tag{7}$$

The zero-time correlations $\phi_{jk}(\mathbf{r},\mathbf{r}'',0) = \langle \delta C_j(\mathbf{r},0) \delta C_k(\mathbf{r}'',0) \rangle$, can be simplified assuming an ideal chemical solution. Under this condition, the positions of different molecules of the same species as well as those of different species must be uncorrelated, and:

$$\langle \delta C_j(\mathbf{r},0) \delta C_k(\mathbf{r}'',0) \rangle = \langle C_j \rangle \delta_{jk} \delta(\mathbf{r} - \mathbf{r}'') \tag{8}$$

Hence, the mean square fluctuation of C_j in a given volume is equal to the mean concentration $\langle C_j \rangle$, as dictated by Poisson statistics.

By inserting eq. 8 into eq. 7, and performing the integration over $\mathbf{r}''$, we arrive at the following equation for the concentration correlation function[1]:

$$\phi_{jl}(\mathbf{r},\mathbf{r}',\tau) = \frac{\langle C_j \rangle}{(2\pi)^3} \int d^3\mathbf{q}\, e^{i\mathbf{q}(\mathbf{r}-\mathbf{r}')} \sum_{s=1}^{m} X_l^{(s)} e^{\lambda^{(s)}\tau} (X^{-1})_j^{(s)} \tag{9}$$

As has been shown elsewhere, this function is symmetric with respect to the indices j and l: $\phi_{jl}(\mathbf{r},\mathbf{r}',\tau) = \phi_{lj}(\mathbf{r},\mathbf{r}',\tau)$ [1].

1.2.2 The normalized intensity correlation function

The normalized intensity correlation function $G(\tau)$ is defined by the fluorescence intensity fluctuations $\delta i(t)$ measured at time t and after time $t+\tau$, averaged over all t, and normalized to the squared mean intensity:

$$G(\tau) = \frac{\langle \delta i(0)\delta i(\tau)\rangle}{\langle i(t)\rangle^2} \tag{10}$$

The intensity fluctuations $\delta i(\tau)$ of component j are proportional to the concentration fluctuations $\delta C_j(\mathbf{r},\tau)$, as well as to the excitation intensity $I(\mathbf{r})$, and the product of the jth component's extinction coefficient and fluorescence quantum yield, Q_j:

$$\delta i(\tau) = \int d^3\mathbf{r} I(\mathbf{r}) \sum_{j=1}^{m} Q_j \delta C_j(\mathbf{r},\tau) s \tag{11}$$

In fact, $I(\mathbf{r})$ describes both the illumination as well as detection properties of the optical setup. For a confocal microscope, $I(\mathbf{r})$ is approximated by a three dimensional Gaussian with the transversal width r_0 and the axial width z_0:

$$I(\mathbf{r}) = \exp\left(-2\left(x^2+y^2\right)/r_0^2\right) \cdot \exp\left(-2z^2/z_0^2\right) \tag{12}$$

Inserting eq. (11) into eq. (10) yields:

$$G(\tau) = \frac{1}{\langle i(t)\rangle^2} \iint d^3\mathbf{r}\, d^3\mathbf{r}'\, I(\mathbf{r}) I(\mathbf{r}') \sum_{jl} Q_j Q_l \phi_{jl}(\mathbf{r},\mathbf{r}',\tau) \tag{13}$$

Because of the symmetry of ϕ, the number of summation terms that actually have to be calculated can be reduced by writing:

$$G(\tau) = \frac{1}{\langle i(t)\rangle^2} \iint d^3\mathbf{r}\, d^3\mathbf{r}'\, I(\mathbf{r}) I(\mathbf{r}') \sum_{j} \sum_{l\le j} (2-\delta_{jl}) Q_j Q_l \phi_{jl}(\mathbf{r},\mathbf{r}',\tau) \tag{14}$$

With eq. (9), this leads to:

[1] With $\int d^3\mathbf{r}''\, e^{i\mathbf{q}\mathbf{r}''} \langle C_j\rangle \delta_{jk} \delta(\mathbf{r}-\mathbf{r}'') = \langle C_j\rangle \delta_{jk} e^{i\mathbf{q}\mathbf{r}}$.

$$G(\tau) = \frac{1}{\langle i(t)\rangle^2} \int d^3\mathbf{q} \sum_j \sum_{l\le j} (2-\delta_{jl}) \\ Q_j Q_l \frac{\langle C_j\rangle}{(2\pi)^3} \sum_{s=1}^{m} X_l^{(s)} e^{\lambda^{(s)}\tau} (X^{-1})_j^{(s)} \iint d^3\mathbf{r}\, d^3\mathbf{r}'\, e^{i\mathbf{q}(\mathbf{r}-\mathbf{r}')} I(\mathbf{r}) I(\mathbf{r}') l \quad (15)$$

With the integral:

$$\iint d^3\mathbf{r}\, d^3\mathbf{r}'\, e^{i\mathbf{q}(\mathbf{r}-\mathbf{r}')} I(\mathbf{r}) I(\mathbf{r}') = (\pi/2)^3\, r_0^2\, z_0\, e^{\left(-r_0^2(q_x^2+q_y^2)/4 - z_0^2 q_z^2/4\right)} \quad (16)$$

and the mean intensity

$$\langle i(t)\rangle = \int d^3\mathbf{r} I(\mathbf{r}) \sum_{j=1}^{m} Q_j \langle C_j\rangle = (\pi/2)^{3/2}\, r_0 \sqrt{z_0} \sum_{j=1}^{m} Q_j \langle C_j\rangle \quad (17)$$

the general form of the normalized intensity correlation is:

$$G(\tau) = \frac{1}{\left(\sum Q_j \langle C_j\rangle\right)^2} \int d^3\mathbf{q}\, e^{\left(-r_0^2(q_x^2+q_y^2)/4 - z_0^2 q_z^2/4\right)} \\ \sum_j \sum_{l\le j} (2-\delta_{jl}) Q_j Q_l \frac{\langle C_j\rangle}{(2\pi)^3} \sum_{s=1}^{m} X_l^{(s)} e^{\lambda^{(s)}\tau} (X^{-1})_j^{(s)} \quad (18)$$

1.2.3 The correlation function in cylindrical coordinates

To simplify the calculation of $G(\tau)$, the integration over $\mathbf{q}$ is performed in cylindrical coordinates, using the substitutions $q_x = q_r \cos q_\phi$, $q_y = q_r \sin q_\phi$, $q_x^2 + q_y^2 = q_r^2$, $dq_x dq_y = r dq_r dq_\phi$. Instead of integrating over q_x and q_y from -∞ to ∞, the integration is performed over q_ϕ and q_r from 0 to 2π and 0 to ∞, respectively. The integral is simplified further by taking into account the fact that the integral is symmetric with respect to q_z. Hence:

$$G(\tau) = \frac{1}{\left(2\pi \sum Q_j \langle C_j\rangle\right)^2} \int_0^\infty dq_r \int_0^\infty dq_z\, r e^{\left(-r_0^2 q_r^2/4 - z_0^2 q_z^2/4\right)} \\ \sum_j \sum_{l\le j} (2-\delta_{jl}) Q_j Q_l \langle C_j\rangle \sum_{s=1}^{m} X_l^{(s)} e^{\lambda^{(s)}\tau} (X^{-1})_j^{(s)} \quad (19)$$

Note that $\mathbf{q}^2 = q_r^2 + q_z^2$ is also replaced in the matrix M.

1.3 Parameter dependence

For the matrix M defining the binding diffusion model (eq. (5)), the integral in eq. (19) cannot be solved analytically but has to be approximated numerically. Figure 2 shows numerical solutions to eq. (19) calculated for different parameter values. In these examples the geometrical parameters are set to $r_0 = 0.2\,\mu\text{m}$ and $z_0 = 4.75\,r_0$, reflecting the optical properties of the experimental setup used in this work. The total concentration of fluorescent proteins is set to $C_{\text{total}} = [A] + [AB] = 78\,\text{nM}$, corresponding to an average of 10 particles in the observation volume. This concentration of fluorescent proteins is typically in encountered in live cell FCS experiments such as those described in the main text. The solutions are shown as a function of the diffusion constant, the dissociation rate constant, and the fraction of unbound proteins, F. Here, F is defined as the average concentration of unbound protein, $[A]$, relative to the total concentration, $C_{\text{total}} = [A] + [AB]$. Based on the law of mass action, F can be expressed as a function of the association and dissociation rate constants:

$$F = \frac{[A]}{C_{\text{total}}} = \frac{k_{\text{off}}}{k_{\text{on}}[B] + k_{\text{off}}} \tag{20}$$

Typical diffusion constants of proteins that are freely diffusing in living cells and are not part of large multi-protein complexes range from $5\,\mu\text{m}^2\,\text{s}^{-1}$ to $50\,\mu\text{m}^2\,\text{s}^{-1}$, while dissociation rate constants of proteins transiently interacting with a macromolecular structure such as chromatin can range from $1\,\text{s}^{-1}$ to $100\,\text{s}^{-1}$ (see for example [2]). In this parameter regime, diffusion and binding kinetics produce two clearly distinguishable components in the autocorrelation curves (figure 2). The first component is dependent on the diffusion constant only and shifts to shorter correlation times when D is increased. The dissociation rate constant only affects the second component that shifts to shorter times when k_{off} is increased. The fraction of unbound proteins determines the relative contribution of the two components to the correlation curve.

To conclude, the binding-diffusion model derived here allows the quantitative analysis of binding reactions between mobile proteins and immobile binding sites by FCS. By fitting this model to experimental data, it should be possible to determine the diffusion constant, the dissociation rate constant, as well as the steady-state fraction of unbound proteins. It is important to point out, that this information can only be reliably gained from curve fitting if the two autocorrelation components are sufficiently well separated and the dissociation rate is within a certain range. If the interaction is highly transient, i.e. k_{off} is very large, the intensity fluctuations are dominated by diffusion and only a single autocorrelation component is visible. In this case, fitting of the binding-diffusion model to the data will not lead to correct estimates for the binding and diffusion parameters because changes in D and k_{off} will compensate each other. If, on the other hand, the interaction is very stable, i.e. k_{off} is very small, bound proteins will eventually reside in the focal volume so long, that they will be bleached. Strong photobleaching results in an artifactual autocorrelation component at long correlation times, which would prevent the correct analysis of the diffusion and binding components.

1.4 Calculation of the apparent interaction strength

In a chemical binding equilibrium, the K_D is defined as

$$K_D = [A][B]/[C] \tag{21}$$

Here, $[A]$ and $[B]$ are the concentrations of unbound binding partners A and B, while $[C]$ is the concentration of the complex between A and B. With the total concentrations $[A]_T = [A] + [C]$ and $[B]_T = [B] + [C]$, eq (21) becomes:

$$K_D = [C]\left(\frac{[A]_T}{[C]} - 1\right)\left(\frac{[B]_T}{[C]} - 1\right) \tag{22}$$

The total concentrations of A and B and the concentration of C are related to the observables of FCCS experiments, the auto- and crosscorrelation amplitudes, in the following way:

$$[A]_T = 1/(G_A V_{\text{eff}}) \tag{23}$$
$$[B]_T = 1/(G_B V_{\text{eff}}) \tag{24}$$
$$[C] = G_X/(G_A G_B V_{\text{eff}}) \tag{25}$$

Here, G_A and G_B are the autocorrelation amplitudes of A and B, G_X is the crosscorrelation amplitude. V_{eff} is the size of the observation volume. For the sake of simplicity, V_{eff} is assumed to be equal for all channels, an assumption that is only approximately correct. Inserting these equations into eq. (22), yields:

$$K_D = \frac{G_X}{V_{\text{eff}}\, G_A\, G_B}\left(\frac{G_A}{G_X} - 1\right)\left(\frac{G_B}{G_X} - 1\right) \tag{26}$$

The calculation of a K_D for protein-protein interactions is complicated by two characteristic features of live cell measurements. First, the interaction takes place in the presence of a potentially large number of competing interactors. Second, in addition to the labelled proteins, which are encoded by the DNA plasmid used for transfection, there is an unknown fraction of unlabelled proteins expressed from their genomic location, which participate in the binding equilibrium. It is therefore not possible to calculate an absolute K_D for the binary interaction of A and B. Hence, crosscorrelation experiments were quantified by calculating a dimensionless *apparent interaction strength* to compare the extent of interaction in different samples. This also allowed to neglect the effect of an impartial overlap of the two observation volumes, which should be the same in all samples. The apparent interaction strength was calculated as the inverse of the K_D, with $V_{\text{eff}} = 1$. The apparent interaction strength was normalized between the highest and lowest mean values observed.

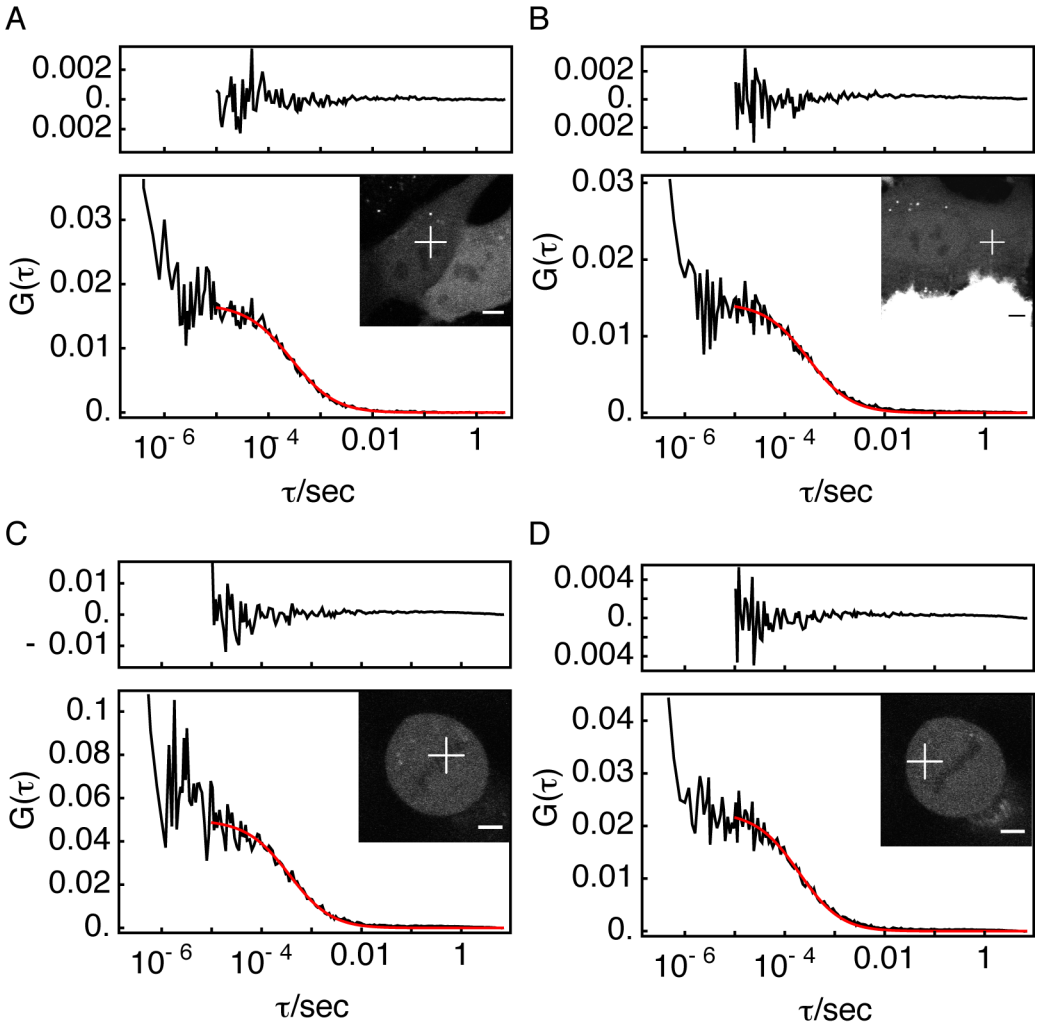

Figure S2: Representative autocorrelation curves of EGFP measured in the nucleus of an interphase HeLa cell (A), the cytoplasm of an interphase HeLa cell (B), on the chromatin of a HeLa cell in metaphase (C), and in the cytoplasm of a HeLa cell in metaphase (D). The measurements were fit with a model of free diffusion (red line). The upper panel shows the fit residuals. The insets show confocal images of the measured cells, where the measurement positions are indicated by white crosses. Scale bars: 5 μm

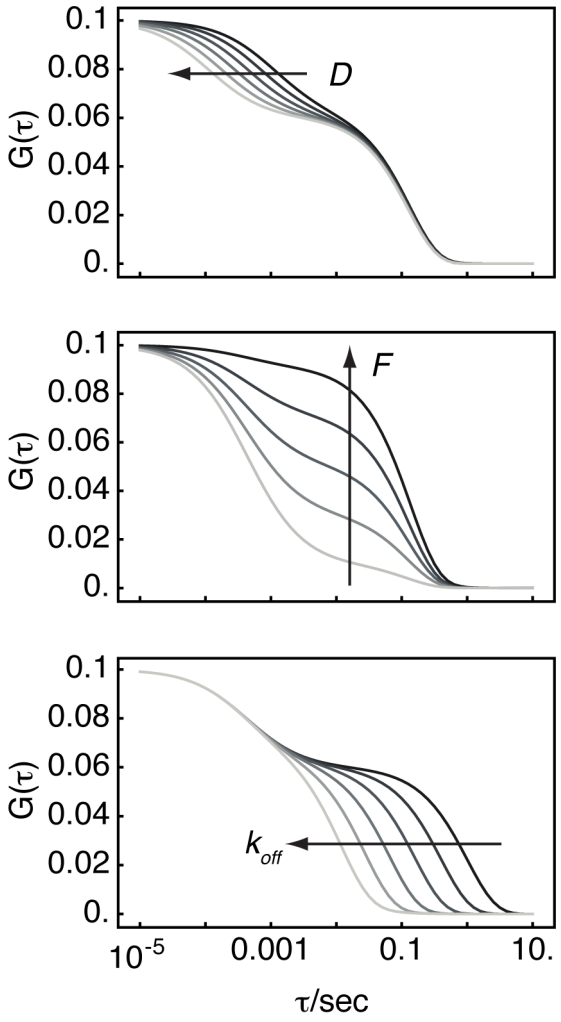

Figure S3: Theoretical autocorrelation curves calculated from the binding diffusion model. The diffusion constant is varied from 5 to 100 μm^2 s^{-1} (top panel), the fraction of unbound proteins is varied from 0.1 to 0.9 (middle), and the dissociation rate constant is varied from 1 to 100 s^{-1} (bottom). In each case the arrow points in the direction of increasing parameter values.

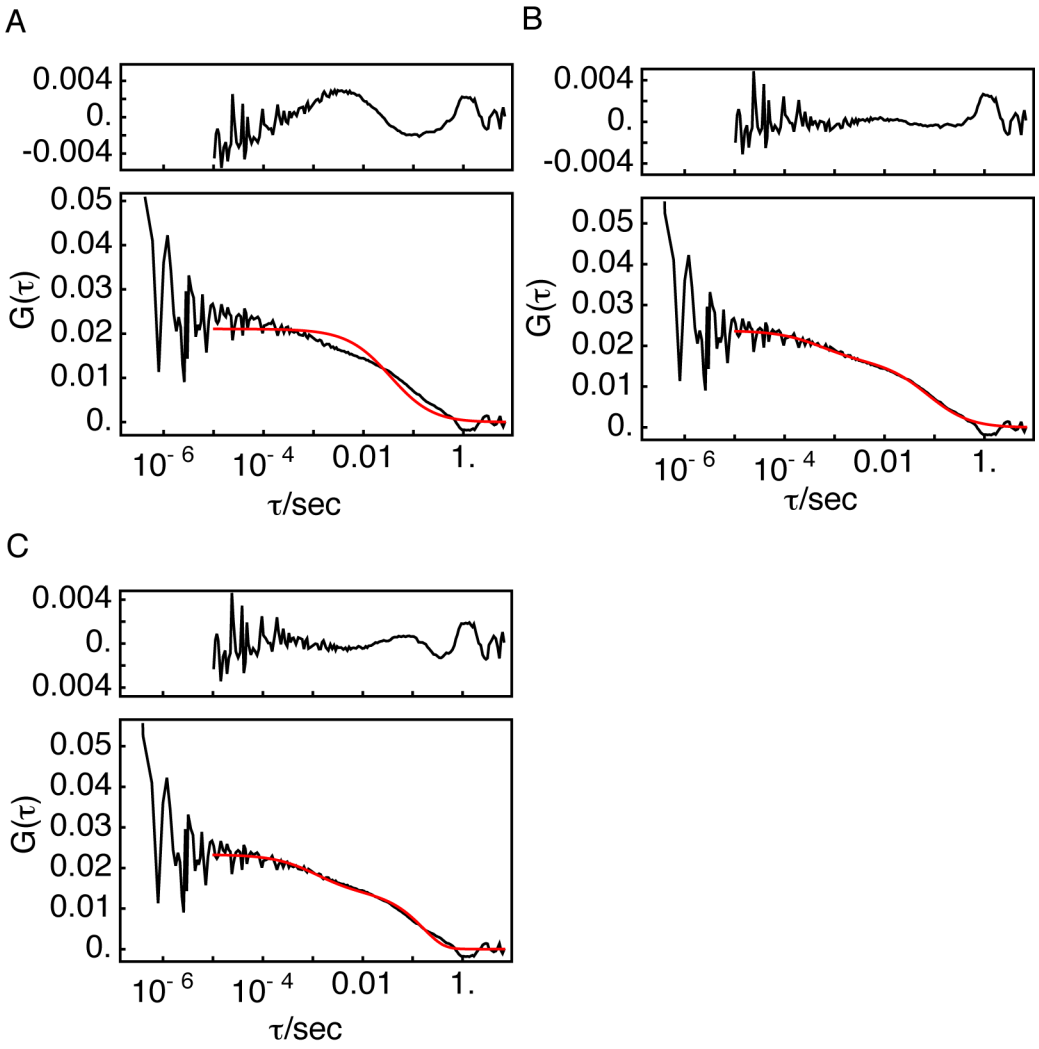

Figure S4: A representative autocorrelation curve of RCC1-EGFP recorded in the nucleus of an interphase HeLa cell, fit with a single component diffusion model (A), a two component diffusion model (B), and the binding diffusion model (C).

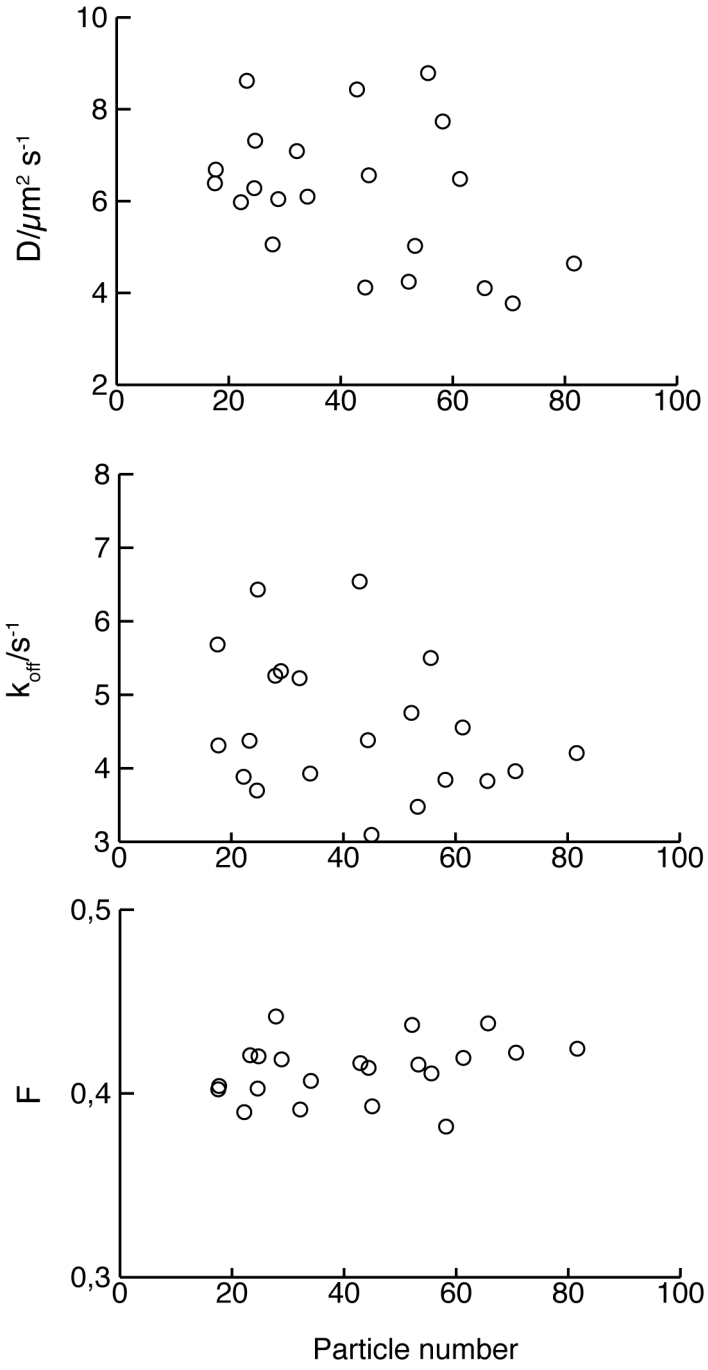

Figure S5: Correlation of the particle number determined for RCC1-EGFP in interphase nuclei and the parameters D, k_{off}, and F. Each circle represents a FCS measurement in an individual cell.

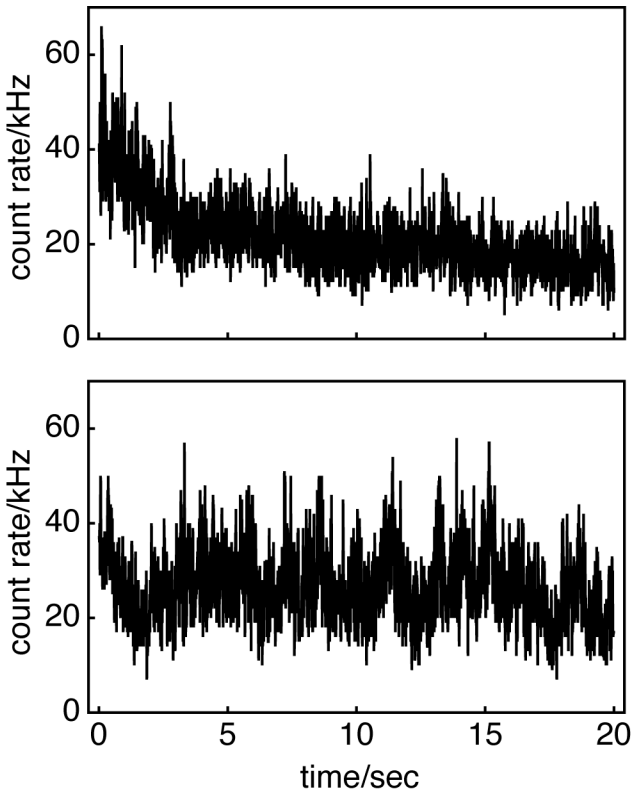

Figure S6: FCS measurements on histone H2B-EGFP show a fast bleaching of the H2B-EGFP fluorescence (top), which indicates that nucleosomes are immobile on the timescale of the FCS experiment. Under the same conditions, the fluorescence of RCC1-EGFP is stable (bottom). Both measurements were taken at the same laser power in nuclei of HeLa cells.

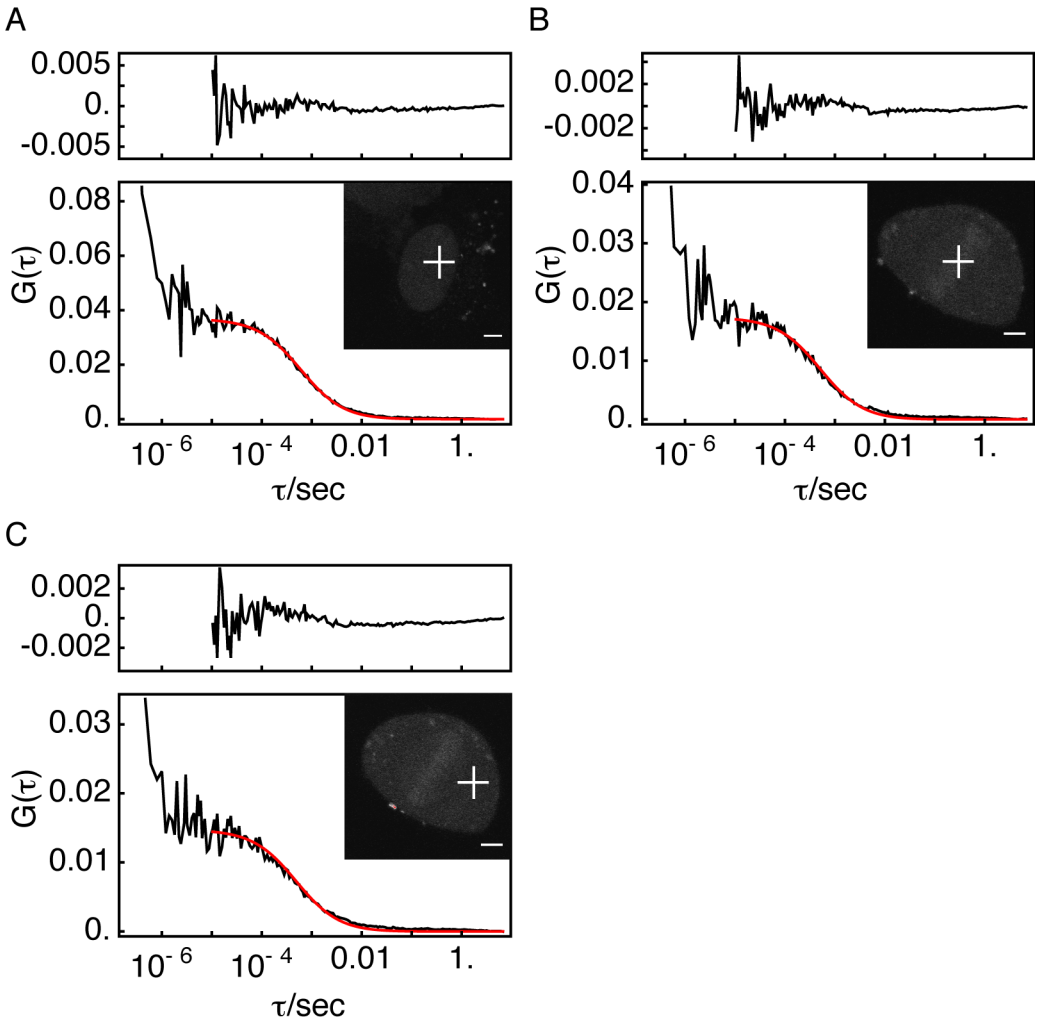

Figure S7: Representative autocorrelation curves of NT-EGFP measured in the nucleus of an interphase HeLa cell (A), on the chromatin of a HeLa cell in metaphase (B), and in the cytoplasm of a HeLa cell in metaphase (C). NT-EGFP refers to a fusion protein comprising the first 27 amino acids of RCC1γ fused to EGFP. All data were fit with a model for free diffusion. The upper panel of each graph shows the fit residuals. Insets show confocal images of the measured cells, where the white crosses indicate the measurement positions. Scale bars: 5 μm.

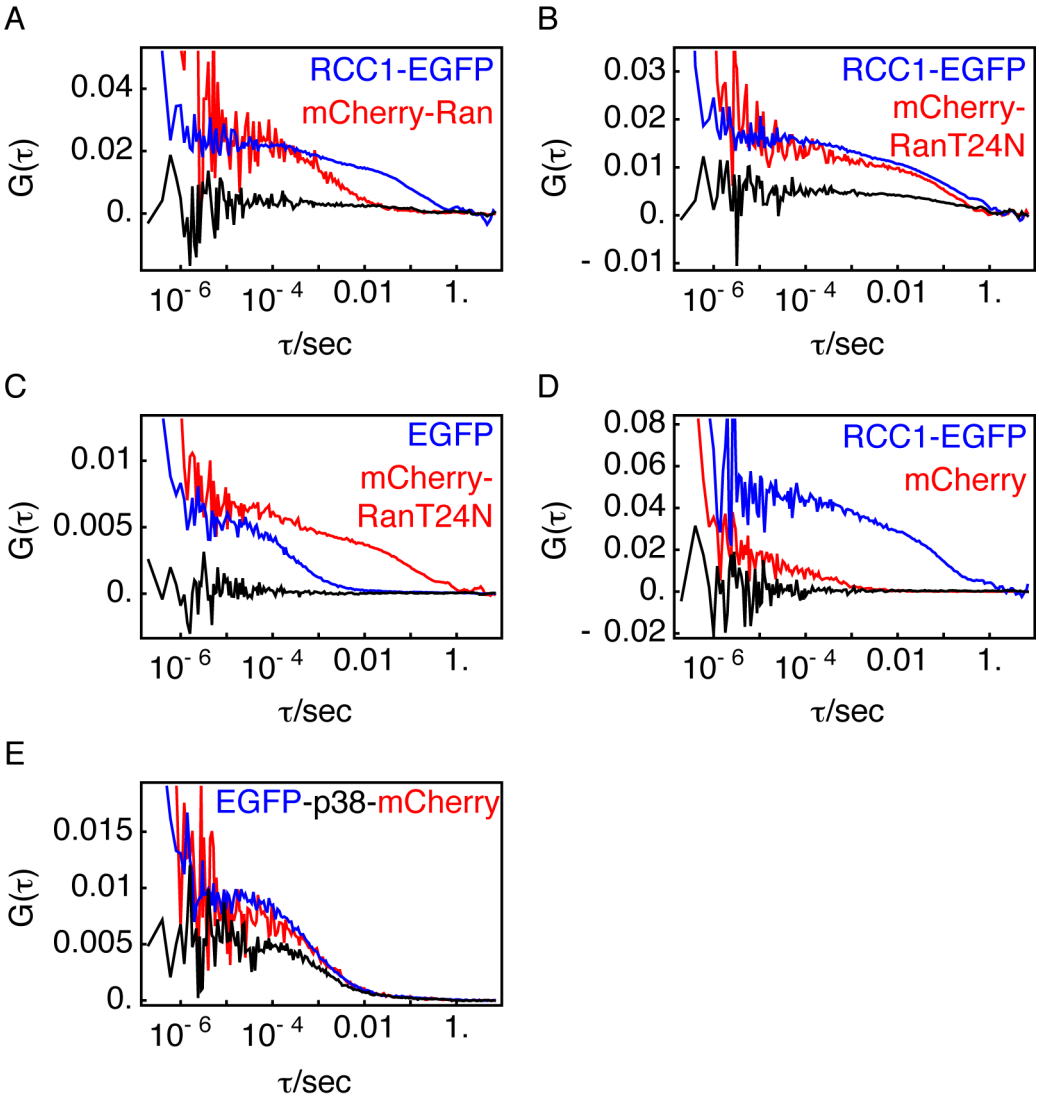

Figure S8: Representative crosscorrelation measurements showing autocorrelation curves of the EGFP channel (blue), the mCherry channel (red), and the cross-correlation curve (black). All measurements were taken in nuclei of interphase HeLa cells coexpressing either RCC1-EGFP and mCherry-Ran (A), RCC1-EGFP and mCherry-RanT24N (B), EGFP and mCherry-RanT24N (C), RCC1-EGFP and mCherry (D), or expressing EGFP-p38-mCherry (E).

Supporting References

[1] E. L. Elson and D. Magde (1974). Fluorescence correlation spectroscopy. I. Conceptual basis and theory. *Biopolymers*, **13**, 1–27.

[2] J. Beaudouin, F. Mora-Bermúdez, T. Klee, N. Daigle, and J. Ellenberg (2006). Dissecting the contribution of diffusion and interactions to the mobility of nuclear proteins. *Biophys J*, **90**, 1878–94.